World Journal of Engineering Research and Technology
WJERT
www.wjert.org
SJIF Impact Factor: 7.029

PHASE SYNCHRONIZATION IN COUPLED NEURONS UNDER EXTERNAL LOW

Hongling Zhuang*

School of Science, Jiangxi University of Science and Technology, Ganzhou, 341000, China.

Article Received on 15/08/2024 **Article Revised on 05/09/2024** **Article Accepted on 25/09/2024**

***Corresponding Author**
Hongling Zhuang
School of Science, Jiangxi University of Science and Technology, Ganzhou, 341000, China.

ABSTRACT

Synchronization of neurons helps maintain certain physiological functions in the brain, and networks of synchronized neurons have been studied extensively, In this paper, based on the ML neuron model, the synchronous firing behavior of coupled neurons under external low-frequency signals is discussed. The synchronous transition between bursting and spikes within the bursting can occur simultaneously. The neurons showed complete synchronization, anti-phase synchronization of spikes within the bursting and bursting, anti-phase synchronization of within the bursting andin-phase synchronization of bursting, and the number of spikes within the bursting increases with the increase of coupling strength. The effect of coupling intensity on neuronal firing was analyzed by the phase difference of spikes, the phase difference of bursting and inter-peak interval (ISI). The pathological changes and disorders of the brain are closely related to the synchronous behavior of neurons, and abnormal synchronization will lead to the occurrence of a variety of nervous system diseases. The research results help us to understand the occurrence of different functions in the human brain and the generation of diseases, and provide a certain basis for brain science.

KEYWORDS: Coupling, ML Model, Spikes Within The Bursting Synchronization, Bursting Synchronization, External input.

1. INTRODUCE

Neural network is a large and complex nonlinear dynamic system, which is an information network formed by many neurons connected by synapses. In order to more truly reflect the

characteristics of the human nervous system, scholars continue to build and improve a variety of types of neuron models, Common examples include Hodgkin-Huxley (HH) model[1], Morris-Lecar (ML) model[2], Hindmarsh-Rose (HR) model[3] and Chay[4] model. Scholars have studied the effects of system parameters on neuron firing and the generation of different firing modes. In the process of information transmission in the whole nervous system, at least two neurons need to form a neural network through coupling to carry out synergistic action, and different topological structures will affect the collective phase synchronization. Phan et al.[5] proposed a partially diffused boundary-coupled HR neural network model and proved that the neural network can achieve asymptotic synchronization when the boundary-coupled strength and stimulus signal exceed the quantization threshold. Wu et al.[6] studied the synchronization of HR neuron model under the action of white Gaussian noise, and the results confirmed that coupling intensity and appropriate noise play a certain role in achieving synchronization of HR neuron model. Juang et al. studied the synchronization of bursting firing in chemical synaptic coupled neural networks, and presented the influencing factors for the existence of stable synchronous bursting.[7] Wang Qingyun et al. established a fast spike neuron model of chemical synaptic coupling to study the effects of key parameters such as synaptic coupling intensity and decay rate on the synchronous behavior of neurons.[8] In addition, the problem of in-phase synchronization and anti-phase synchronization considering synaptic delay.[9,10] Dha mala et al. built a mathematical model of Hindmash-Rose (H-R) neurons with electrical synaptic coupling, and found that the bursting firing synchronization corresponding to spike firing was earlier.[11] The synchronized behavior of neurons helps us understand how brain information is transmitted and processed, and the analysis of the collective dynamics of these neural networks is critical for practical applications, such as treating Parkinson's disease, Alzheimer's disease, and epilepsy. Many studies have shown that the pathological changes and disorders of the brain are closely related to the synchronous behavior of neurons.[12,15] In the past few years, neuronal phase synchronization has become a significant subject in the study of neural activity.[16,23]

In this paper, the bursting and synchronization behavior of electrically coupled neurons under external low frequency is studied, and the influence of coupling strength on synchronization behavior is discussed. The phase difference of spikes within the bursting, the phase difference of burstings and the interpeak interval (ISI) are used to analyze. The results show that with the increase of the coupling intensity, the firing behavior of the spikes within

the bursting changes from in-phase synchronization to anti-phase synchronization, and the bursting also transition. The synchronous transition between bursting and spikes within the bursting can occur simultaneously. In addition, the number of firing spikes of coupled neurons increases with the increase of coupling intensity. This result is helpful for us to understand the occurrence of different functions in the human brain and the generation of diseases, and is also one of the foundations and keys to explore the field of brain science, especially the information processing and transmission in the brain.[24,25]

2. SINGLE NEURON MODEL UNDER EXTERNAL SIGNAL

The electrical activity of crustacean muscle fibers is modeled by the ML neuron model. It is a simpler variant of the HH neuron model. The rapid activation variable *v* (membrane voltage) in the model, a variable *w* that recovers more slowly. *v* denotes the voltage (expressed in mV) and determines the instantaneous activation of the fast current (*ifast*), and the function *w* governs the activation of the slower current (*islow*), which is a function of *v*. $c\frac{dv}{dt}$ is the capacitor's current flowing in response to variations in the ion density on the film's inner and outer surfaces. The flow of charged particles through ion channels is characterized by the ionic currents *ileak*, *islow*, and *ifast*. Each ion channel opens and closes, causing the charged particles to flow in this process. *c* stands for membrane capacity, and i_{stim} for external input current. Lastly, the equation that follows provides the model

$$\begin{aligned} c\frac{dv}{dt} &= i_{stim} - i_{fast} - i_{leak} - i_{slow} \\ \frac{dw}{dt} &= \varphi \frac{m_2(v) - w}{b(v)} \end{aligned} \tag{1}$$

With

$$\begin{aligned} i_{fast} &= g_{fast} m_1(v)(v - e_{NA}) \\ i_{leak} &= g_{leak}(v - e_{leak}) \\ i_{slow} &= g_{slow} w(v - e_K) \end{aligned}$$

The parameters *eNA*, *eK*, and *eleak* represent the equilibrium potential of *Na*+, *K*+, and leaking ions, while *gfast*, *gslow*, and *gleak* represent the maximum conductivity of the corresponding ionic current. They reflect the density of ion channels distributed on the membrane. The control parameter □ controls the rate of change of *w*. Steady state $m1$ and $m2$ are nonlinear functions of *v*, as follows:

$$m_1(v) = 0.5(1 + \tanh\frac{v - u_1}{u_2})$$

$$m_2(v) = 0.5(1 + \tanh\frac{v - u_3}{u_4})$$

$$b(v) = \frac{1}{\cosh\frac{v - u_3}{2u_4}}$$

The activation midpoint potentials are represented by the values $u1$ and $u3$, and the corresponding current is the current in the semi-activated state, $u2$ and $u4$ represent the slope factor of activation, b is the time constant of potassium ion activation. The neurons are stimulated by periodic sinusoidal signals with external excitation to study different discharge behaviors, That is, $istim=A\sin(\omega t)$, when the frequency ω is changed, the firing mode of neurons will change. For very low frequency stimulation, the neurons fire periodically, and there will be n peak bursts, every stimulation cycle with n pulse bursts indicates that there are n action potentials. The neurons showed cluster firing behavior.

Taking the external excitation amplitude A=5 and select different frequencies, as shown in Fig.1(a-d). When ω=0.02, the neuron will have a bursting firing mode of period 16, when ω=0.04, the neuron will have a bursting firing mode of period 6, when ω=0.06, the neuron will have a bursting firing mode of period 3, when ω=0.3, the neuron will have a peak firing mode.

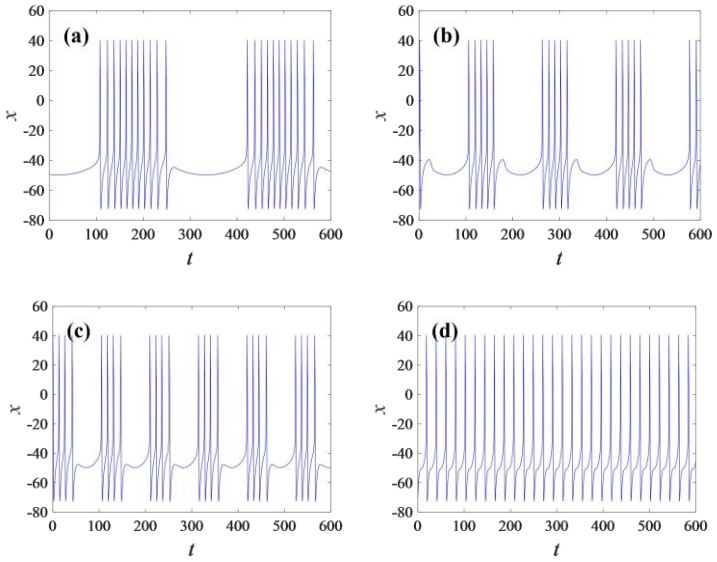

Fig. 1: Time sequence diagram of a single ML neuron for ω. (a) ω=0.02, (b) ω=0.04, (c) ω=0.06, (d) ω=0.3.

As shown in Fig 2 (a), it reflects the variation trend of ISI between peaks and peaks when the external frequency ω changes from 0 to 0.3, and Fig.2(b) is a local magnification within the box of Fig.2(a). It can be visually seen that ISI is very densely distributed in the front, and there are more peak-to-peak periods, that is, there are multiple action potentials in the bursting. As the frequency ω increases, the neuron gradually changes from multi-cycle bursting firing pattern to cycle 3, cycle 2 firing pattern, until it shows a single cycle of spike firing.

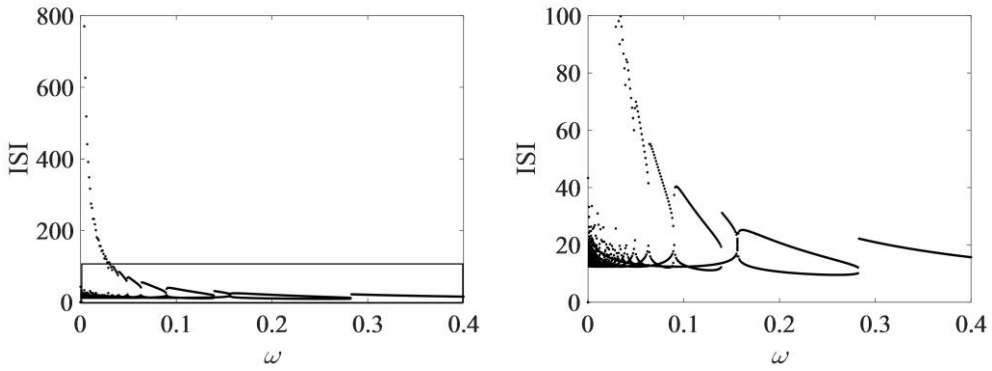

Fig. 2: (a) ISI bifurcation diagram of ω, (b) Locally enlarged image.

3. COUPLED NEURON MODEL AND NUMERICAL RESULT

In order to further study the firing synchronization behavior between neurons under electrical synaptic coupling, the constructed electrically coupled ML neurons can be expressed as:

$$
\begin{aligned}
c\frac{dv_1}{dt} &= i_{stim} - i_{1,fast} - i_{1,leak} - i_{1,slow} - k(v_2 - v_1) \\
\frac{dw_1}{dt} &= \varphi\frac{m_2(v_2) - w_1}{b(v_1)} \\
c\frac{dv_2}{dt} &= i_{stim} - i_{2,fast} - i_{2,leak} - i_{2,slow} - k(v_1 - v_2) \\
\frac{dw_2}{dt} &= \varphi\frac{m_2(v_2) - w_2}{b(v_2)}
\end{aligned}
\qquad (2)
$$

Where k represents the electrical connection gap between neurons, and other parameter values are given in Table 1.

Table 1: Each parameter value of ML model.

*u*1 *u*2	-1.2mV 18mV	*gfast* *gslow*	20mS/cm^2 20mS/cm^2	*eNa* *eK*	50mV -100mV	ϕ *c*	0.15 2u
*u*3	-13mV	*gleak*	2mS/cm^2	*eleak*	-70mV		
*u*4	10mV						

To investigate the effect of coupling strength on the synchronous firing of neurons by coupling two neurons in a bursting firing under low frequency signals. Fixed external sinusoidal amplitude A=5, frequency ω=0.035, further study the phase synchronization between the firing of the two neuronal burstings, and concentrate on the weak coupling range. When the coupling intensity k=0.05, according to the figure 3(a)-(b), the timing diagram and phase diagram match. It can be seen from the figure that the red line and blue line of the timing diagram are completely coincident, and the phase diagram is a straight line, at which time the two neurons are in complete synchronization.

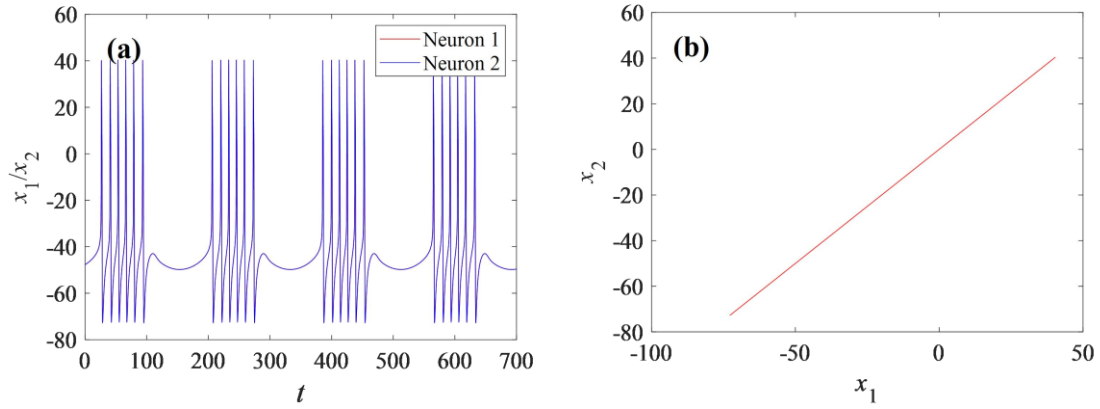

Fig. 3: (a) Membrane potential time series diagram, (b) Diagram of the phase trajectory in the $x1$-$x2$ plane.

As the coupling strength increases even more, the neurons present different synchronous dynamic behaviors. It is obvious in Fig. 4(a) that when the coupling strength is weak (k=0.11), the two neurons are still completely synchronized. Then, as the coupling strength increases, spikes within the bursting begins to show high-pulse and low-pulse firing patterns. For example, coupling intensity k=0.135, as shown in Fig.4(b), in-phase synchronous firing of neuronal spikes within the bursting gradually shifts to anti-phase synchronous firing. When coupling intensity is k=0.15 and k=0.16 respectively, as shown in Fig.4(c-d), the anti-phase synchronous range of spikeswithin the bursting gradually increases, while the in-phase synchronous range gradually decreases. It is not until the coupling strength increases to a certain strength that the firing behavior of the spikes within the bursting completely changes to the anti-phase synchronous state.

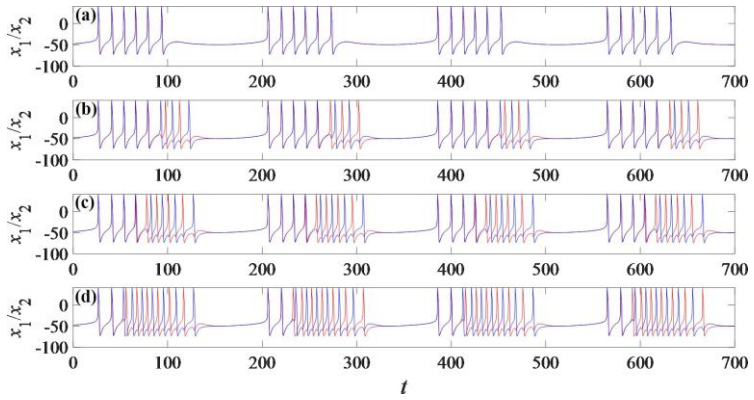

Fig. 4: Time series of membrane potential of coupled neurons. (a) *k*=0.11, (b) *k*=0.135, (c) *k*=0.15, (d) *k*=0.16.

When the coupling intensity is further increased to *k*=0.18, as shown in Fig. 5(a), coupled neurons transition to anti-phase synchronization between bursting and spikes within the bursting. Each bursting of neuron 1 contains 10 high-amplitude spikes, while each bursting of neuron 2 contains 9 high-amplitude spikes, where the spikes within the bursting forms anti-phase synchronization between the two coupled neurons. The spikes within the bursting alternated between high and low amplitude. When *k*=0.19, as shown in Figure 5(b), each bursting has the same number of high-amplitude spikes (n=10), and the coupled neuron bursting transitions from antiphase synchronization to in-phase synchronization, while the spikes within thebursting still maintain antiphase synchronization between the two coupled neurons.

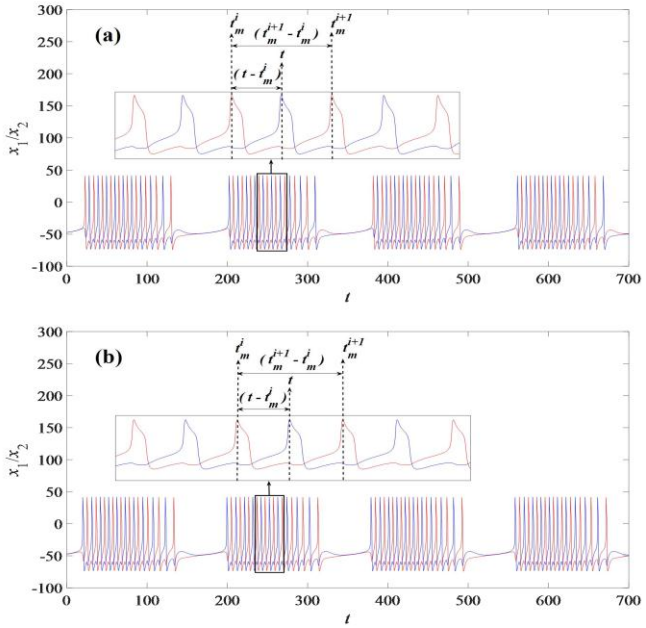

Fig. 5: Time series diagram of membrane potential of coupled two neurons. (a) *k*=0.18, (b) *k*=0.19.

The spikes within the bursting firing of the neurons can be clearly represented in the inset of Figure 5(a) (b), where the in-phase synchronization of the burstings and the anti-phase synchronization of the burstings are more clearly represented by the separate time series of the two coupled neurons in Figure 6. The red line represents neuron 1, and the blue line represents neuron 2. When k=0.18, the coupled neurons exhibit two types of bursting firing modes, which leads to an antiphase synchronization in the bursting firing; when k=0.19, the coupled neurons have only one type of bursting firing mode, which is an in-phase synchronization in the cluster firing. For convenience, the stages of the spikes within the bursting are defined as follows:

3.1 Spike phase function and phase difference of coupled neurons

The spike phase function of coupled neurons m(m=1,2) is typically used to describe synchronization. The expression for the spike phase function $\theta(t)$ is as follows:

$$\theta_m(t) = 2\pi \frac{t - t_m^i}{t_m^{i+1} - t_m^i} + 2\pi i, \quad (t_m^i < t < t_m^{i+1},\ i = 1,2,\ldots,N-1), \tag{3}$$

Where t is the time, t_m^i the firing time of the i-th spike of neuronal m (m=1,2), and N is the number of spikes. The phase difference between spikes is defined as: $\Delta\theta(t) = |\theta_1(t) - \theta_2(t)|$, Defining phase synchronization based on the value of $\Delta\theta(t)$: (1) $\Delta\theta(t) = 0$, The spikes are in-phase synchronized; (2) $\Delta\theta(t) = \pi$, The spikes are anti-phase synchronized.

3.2 Bursting phase function and phase difference of coupled neurons

Consistent with the spike phase function, the bursting phase function $\Delta\theta^*(t)$ of coupled neurons m (m=1,2) is defined as follows

$$\theta^*{}_m(t) = 2\pi \frac{t - T_m^i}{T_m^{i+1} - T_m^i} + 2\pi i, \quad (T_m^i < t < T_m^{i+1},\ i = 1,2,\ldots,M-1), \tag{4}$$

Where t is the time, T_m^i is the peak time of the first spike of each larger bursting i (For example, in Figure 6, a cycle consists of 10-spikes bursting and 9-spikes bursting) is the firing time of the first peak of bursting i of neuron m(m =1,2), and $M$is the number of burstings. The phase difference between burstings is defined as: $\Delta\theta^*(t) = |\theta_1^*(t) - \theta_2^*(t)|$, Defining phase synchronization based on the value of $\Delta\theta^*(t)$: (1) $\Delta\theta^*(t) = 0$, The burstings are in-phase

synchronized, (2) $\Delta\theta^*(t)=\pi$, The burstings are anti-phase synchronized.

To see the anti-phase synchronization of the burstings more clearly, the timeseries of the two coupled neurons are presented separately in Fig.6 at *k*=0.19. Clearly, the time series consists of alternating burstings containing 10 spikes (solid boxes) and 9 spikes (dashed squares). In addition, because neuron 1 is in the 10-spike bursting and neuron 2 is in the 9-spike bursting, there is an anti-phase synchronization in the bursting. The phase difference $\Delta\theta^*(t)=\pi$ of the system bursting of coupled neuronal oscillations is obtained. At this time, the bursting firing of the coupled nervous systemis in the anti-phase synchronization state.

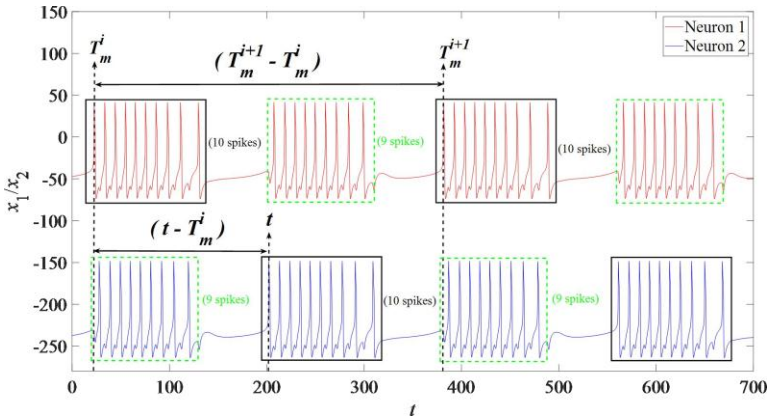

Fig. 6: Time series of neurons 1(red) and 2(blue).

In addition, the peak-interval bifurcation analysis of coupled neurons was carried out by changing the coupling strength, and the influence of coupling strength on neuron firing pattern was observed. The ISI bifurcation of coupling strength *k* is shown in Fig. 7(a). Obviously, it can be observed that the coupling strength has the same firing mode in the range (*k*=0~0.135), in which the two neurons are in a completely synchronous state. With the rise in coupling strength, the two neurons change from the same firing mode to different firing mode, and there are periodic firing mode and chaotic firing mode in this change process. Neurons change from in-phase toanti-phase synchronization. Figure 7(b) shows the local magnified bifurcation diagram for coupling strength 0.1 to 0.2.

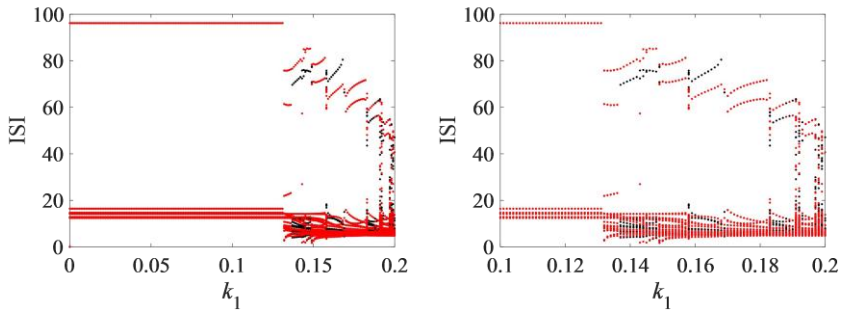

Fig. 7: (a) ISI bifurcation diagram of coupling strength, (b) Local magnification.

Then, the transition process with the rise in coupling strength can be clearly observed through the phase difference between the spikes within the bursting and the bursting. As shown in Figure 8, when k=0.17~0.182, the phase difference between burstings and spikes within the bursting is both $\Delta\theta = \pi,\ \Delta\theta^* = \pi$; when k=0.183~0.19, the phase difference between spikes within the bursting is still $\Delta\theta = \pi$, while the phase difference of burstings is $\Delta\theta^* = 0.03$, and the phase difference decreases from π to 0.03. During this period, the firing behavior of the coupled neurons changed from anti-phase synchronization to in-phase synchronization, but the spikes within thebursting keep anti-phase synchronization.

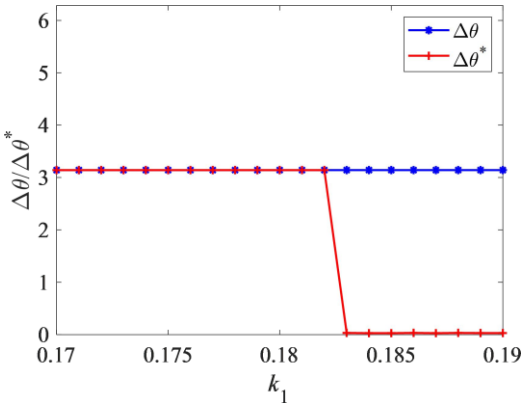

Fig. 8: The phase difference between the spikes within the bursting and the bursting.

In addition, increased coupling strength not only changes the synchronous changes of the two neurons, but also changes the number of neuronal firing spikes. Asshown in Figure 9, when the coupling strength is weak, the coupling neurons are in a completely synchronous state, and the number of spikes within the bursting remains unchanged. When the coupling strength is greater than a certain threshold, the number of spikes within the bursting also begins to change. As shown in Figure 9, which clearly shows that the number of spikes within the bursting increases gradually with the increase of the coupling strength.

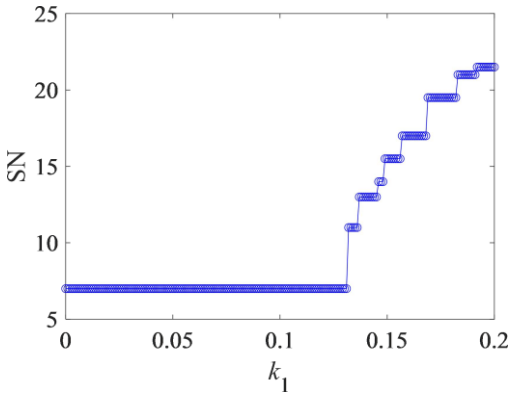

Fig. 9: The number of spikes within the bursting.

4 CONCLUSION

In this paper, we investigated the synchronous firing behavior of electrically coupled neurons in response to external low-frequency signals based on the ML neuron model. For the synaptic coupling neuron system, when the coupling intensity is small, the membrane potential curves of the two neurons are completely overlapped,that is, the coupling neurons in a completely synchronous state. Further increasing the coupling strength, the spikes within the bursting firing of neurons gradually transition from complete synchronization to anti-phase synchronization, until the coupling strength is greater than a certain threshold, the whole spikes within the bursting firing of neurons transition to anti-phase synchronization. In addition, the bursting firing of neurons also changes between in-phase synchronization and anti-phase synchronization. During the whole process, neurons appear complete synchronization, the spikes within the bursting and burstings are anti-phase synchronized, anti-phase synchronization of spikes within the bursting and in-phase synchronization of burstings. However, the number of spikes within the bursting increase with the increase of coupling strength. Synchronization between neurons plays a crucial role in cognitive processes such as sensation, learning, memory and thinking, but abnormal synchronization can lead to a variety of neurological diseases, such as epilepsy, Alzheimer's, schizophrenia, Parkinson's and other diseases. Therefore, the analysis of neuronal synchronization is crucial for understanding the information transmission and processing process in the brain, and has great significance for understanding brainfunction and disease mechanism.

5 REFERENCE

1. HODGKIN A L, Huxley A F.A quantitative description of membrane current and its application to conduction and excitation in nerve [J]. The Journal of Physiology, 1952; 117(4): 500–544.

2. MORRIS C, LECAR H. Voltage oscillations in the barnacle giant muscle fiber[J]. Biophysical Journal, 1981; 35(1): 193-213.
3. HINDMARSH J L, ROSE R M. A model of Neuronal Bursting Using Three Coupled First Order Differential Equations [J]. Proceedings of the Royal Society B: Biological Sciences, 1984; 221(1222): 87-102.
4. CHAY T R, FAN Y S, LEE Y S .Bursting, Spiking, Chaos, Fractals and Universality in Bi ological Rhythms [J]. International Journal of Bifurcation & Chaos, 1995; 5(03): 595-635.
5. PHAN C, YOU Y C. Synchronization of boundary coupled Hindmarsh–Rose neuron network [J]. Nonlinear Analysis: Real World Applications, 2020; 55: 103139.
6. WU K J, WANG T J. Study On electrical synapse coupling synchronization of Hindmarsh -Rose neurons under Gaussian white noise [J]. Neural Computing & Applications, 2018; 30(2): 551-561.
7. Juang J, Liang Y H. Cluster synchronization in networks of neurons with chemical synapses [J]. Chaos: An Interdisciplinary Journal of Nonlinear Science, 2014; 24(1).
8. Wang Q, Lu Q, Chen G. Synchronization transition induced by synaptic delay in coupled fast-spiking neurons[J]. International Journal of Bifurcation and Chaos, 2008; 18(04): 1189-1198.
9. Bär M, Schöll E, Torcini A. Synchronization and complex dynamics of oscillators with delayed pulse-coupling[J]. Angew. Chem. Int. Ed, 2012; 51: 9489-9490.
10. Jörg D J, Morelli L G, Ares S, et al. Synchronization dynamics in the presence of coupling delays and phase shifts[J]. Physical Review Letters, 2014; 112(17): 174101.
11. Dhamala M, Jirsa V K, Ding M. Transitions to synchrony in coupled bursting neurons [J]. Physical Review Letters, 2004; 92(2): 028101.
12. Uhlhaas J P, Singer W. Neural Synchrony in Brain Disorders: Relevance for Cognitive Dysfunctions and Pathophysiology [J]. Neuron, 2006; 52(1).
13. Tass, Peter, et al. "Detection of n: m phase locking from noisy data: application to magnetoencephalography." Physical review letters, 1998; 81(15): 3291.
14. V O P, Christian H, A P T. Effective desynchronization by nonlinear delayed feedback. [J]. Physical review letters, 2005; 94(16).
15. Alfons S, Joachim G. Normal and pathological oscillatory communication in the brain. [J]. Nature reviews. Neuroscience, 2005; 6(4).
16. Zhao Y, Ping Z, Zhigang Z, et al. Phase synchronization between a light-dependent neuron and a thermosensitive neuron [J]. Neurocomputing, 2020 (prepublish).

17. C T, O B, C F. Oscillatory synchrony between human extrastriate areas during visual short-term memory maintenance. [J]. The Journal of neuroscience: the official journal of the Society for Neuroscience, 2001; 21(20).
18. N Y K, B K B, E S. Amplitude and phase dynamics in oscillators with distributed-delay coupling. [J]. Philosophical transactions. Series A, Mathematical, physical, and engineering sciences, 2013; 371(1999).
19. Roux F, Uhlhaas J P. Working memory and neural oscillations: alpha–gamma versus theta–gamma codes for distinct WM information?[J]. Trends in Cognitive Sciences, 2014; 18(1).
20. Jonathan D, Thomas G, K A E, et al. Phase-Amplitude Coupling and Long-Range Phase Synchronization Reveal Frontotemporal Interactions during Visual Working Memory. [J]. The Journal of neuroscience: the official journal of the Society for Neuroscience, 2017; 37(2).
21. V M I, V G O, D V S, et al. Phase synchronization in ensembles of bursting oscillators.[J]. Physical review letters, 2004; 93(13).
22. Haitao Y, Jiang W, Bin D, et al. Chaotic phase synchronization in small-world networks of bursting neurons. [J]. Chaos (Woodbury, N.Y.), 2011; 21(1).
23. Xiaojuan S, Matjaž P, Jürgen K. Effects of partial time delays on phase synchronization in Watts-Strogatz small-world neuronal networks. [J]. Chaos (Woodbury, N.Y.), 2017; 27(5).
24. Emilio S, Terrence J, Sejnowski. Correlated neuronal activity and the flow of neural inf ormation[J]. Nature Reviews Neuroscience, 2001; 2(8): 539-550.
25. Golomb D, Rinzel J.Clustering in globally coupled inhibitory neurons[J]. Physica. D: Nonlinear Phenomena, 1994; 72(3): 259-282.